Inorganic Chemistry

Article

pubs.acs.org/IC

Synthesis and Modular Structural Architectures of Mineralogically Inspired Novel Complex Pb Oxyhalides

Oleg I. Siidra,* Diana O. Zinyakhina, Anastasiya I. Zadoya, Sergey V. Krivovichev, and Rick W. Turner†

Department of Crystallography, Saint-Petersburg State University, University emb. 7/9, St. Petersburg, 199034 Russia

Supporting Information

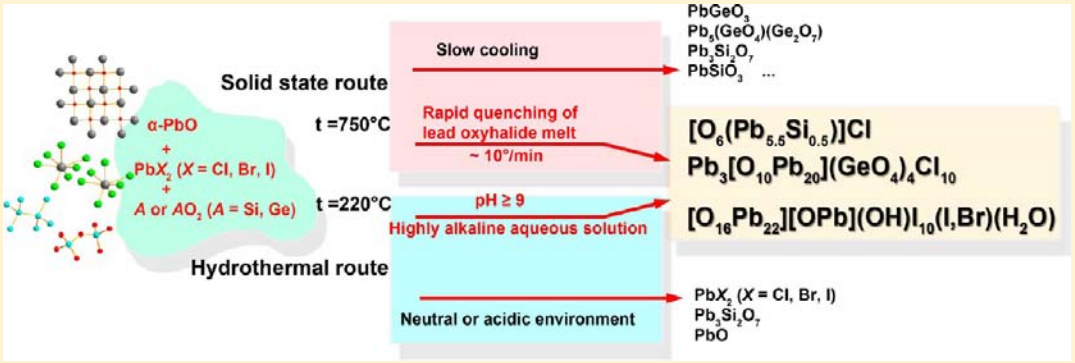

ABSTRACT: Three novel Pb oxyhalides, $Pb_3[O_{10}Pb_{20}](GeO_4)_4Cl_{10}$ (**1**), $[O_{16}Pb_{22}][OPb](OH)I_{10}(I,Br)(H_2O)$ (**2**), and $Pb_{5.5}Si_{0.5}O_6Cl$ (**3**), have been prepared by high-temperature solid-state reactions (**1** and **3**) and hydrothermal method (**2**). The structure of **1** is based upon novel $[O_{10}Pb_{20}]^{20+}$ layers of edge- and corner-sharing oxocentered OPb_4 tetrahedra with cavities occupied by the GeO_4 tetrahedral anions. The interlayer space contains low-occupied Pb sites and Cl^- anions. The structure of **2** contains unique $[O_{16}Pb_{22}][12+]$ layers of edge-sharing OPb_4 tetrahedra with X^- ions (X = I, Br) in and in between the layers. The structure of **3** is the first example of the Pb oxyhalide with the 3:1 ratio between the O−Pb and X sheets (X = halide). The unprecedented structure topologies and architectures observed in the title compounds are closely related to those observed in rare natural Pb oxyhalides that have no synthetic analogues to date.

INTRODUCTION

Pb oxyhalides are of interest due to their environmental[1] and technological[2] importance. They are also known as important constituents of oxidation zones of mineral deposits.[3] Most Pb oxyhalides have layered α-PbO-derivative structures, which are related to the Aurivillius phases.[4] The crystal structures of PbO-related layered lead oxyhalides are based upon the O−Pb layers alternating with the X sheets of X^- ions (X = Cl, Br, I). There is always only one X layer which alternates with one O−Pb (n = 1) or two O−Pb (n = 2) layers, resulting in the O−Pb:X ratios equal to 1:1 and 2:1, respectively (Figure 1b,c). No other stacking sequences have been reported to date. In this respect, the family of PbO-derivative layered structures differs from the huge family of the $Bi_2O_2A_{n-1}B_nO_{3n+1}$ Aurivillius compounds, where one $[Bi_2O_2]^{2+}$ layer alternates with $n$$ABO_3$ (n = 1−7) perovskite octahedral layers.[5] The PbO-derivative compounds may also incorporate a wide range of elements, including As, S, V, Mo, W, P, Si, etc.,[3h,i] which results in interesting chemical and structural diversity and complexity. The relationships between the structures of α-PbO[6] and its oxyhalide derivatives can be conveniently described in terms of structural units based upon OPb_4 oxocentered tetrahedra.[7] Transformation of the [OPb] layer in α-PbO into one of its derivatives corresponds to the removal of blocks of the OPb_4 tetrahedra from the former (Figure 2a). The resulting layers have the chemical composition $[Pb_mO_n]^{z+}$, with $m > n$. The role of the X sheets is to compensate for the positive charge of the O−Pb layers. However, a number of additional modifications have been observed recently.[3h,i] Despite the large amount of synthesized Pb oxysalts with PbO-derivative layers, most of them are limited to rather simple structural architectures.[8] The same is true for the majority of synthetic Pb oxyhalides, whereas chemically similar phases crystallized in natural systems possess very complex structural topologies. Thus, the discovery and preparation of new phases that adopt highly defect and complex PbO-derivative layers remains a challenge. The existence of very complex Pb oxychloride minerals with highly defect PbO-derivative cationic layers in nature inspired us to develop the synthetic routes to obtain similar phases with controlled size and shape of defects.

Herein we report on the studies of the PbO−PbX_2−Ge/SiO_2 and PbO−PbX_2−H_2O (X = Cl, Br, I) systems. Two novel compounds were obtained in these systems by rapid quenching of lead-oxyhalide melt, and the third one was obtained by hydrothermal reactions at rather high pH values. The three new compounds described here illustrate the complexity of the

Received: August 11, 2013
Published: October 11, 2013

   dx.doi.org/10.1021/ic402066h | *Inorg. Chem.* 2013, 52, 12799−12805

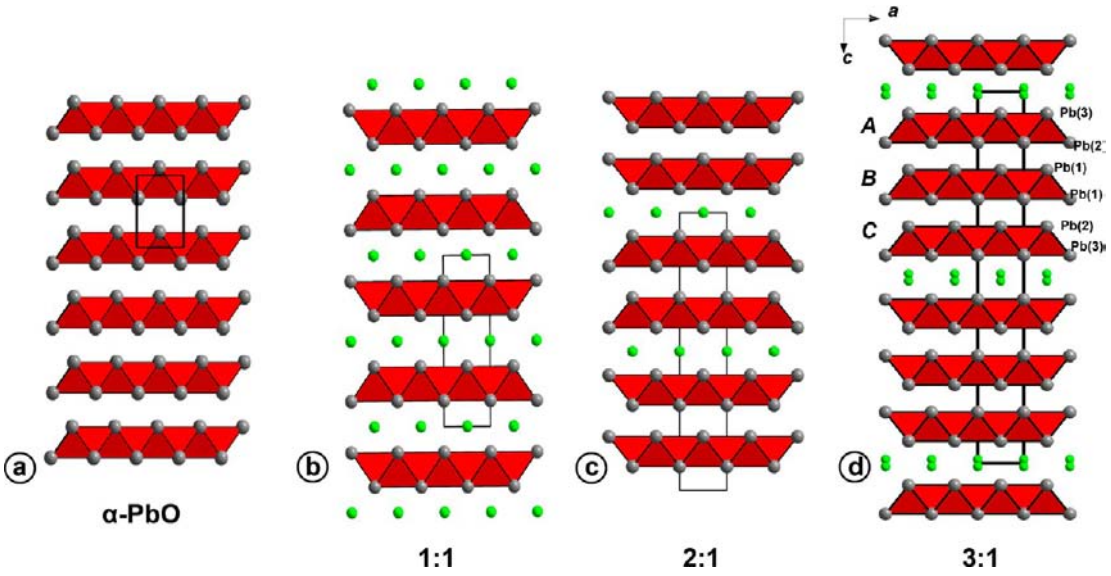

Figure 1. General projection of the crystal structure of α-PbO (a) and representation of structural architectures of 1:1 (b) and 2:1 (c) lead oxyhalides containing PbO blocks and tetragonal *X* sheets of halide ions (*X* = Cl, Br, I) (designations: green balls = halogen atoms, gray balls = Pb^{2+}, red = OPb_4 tetrahedra). General projection of the crystal structure of **3** along *b* axis. See the text for details.

system and validate new pathways for synthesis of complex Pb oxyhalides.

EXPERIMENTAL SECTION

Syntheses. *$Pb_3[O_{10}Pb_{20}](GeO_4)_4Cl_{10}$ (**1**).* α-PbO (powder, ≥99.999%, Aldrich), $PbCl_2$ (powder, 98%, Aldrich), and Ge metal (powder, ≥99.999%, Aldrich) reagents in 0.3:1.5:0.05 ratio were used to obtain single crystals of **1**. The mixture was ground in an agate mortar under acetone and after drying loaded into a platinum crucible and kept at 750 °C for 1 h in air, followed by cooling to 25 °C at a cooling rate of 2.5 °C/min. The product consisted of light-green elongated crystals of **1**. It is of interest that cooling of the same mixture down to room temperature at a lower cooling rate of 5 °C/h results in the formation of transparent yellowish crystals of $PbGeO_3$[9] and $Pb_5Ge_3O_{11}$.[10]

*$[O_{16}Pb_{22}][OPb](OH)I_{10}(I,Br)(H_2O)$ (**2**).* Crystals of **2** were obtained by the hydrothermal method from aqueous solution using the mixture of α-PbO (powder, ≥99.999%, Aldrich), PbI_2 (powder, 99.999%, Aldrich), and $PbBr_2$ (powder, 99.999%, Aldrich) taken in the ratio of 2.3:1:0.2 and 8 mL of distilled H_2O. The pH of solution was adjusted to 9 by the addition of 0.003 g of NaOH. The reactants were placed in a 23 mL Teflon-lined steel autoclave and heated to 220 °C for two days. The autoclave was allowed to cool slowly to room temperature over 24 h. The resulted lemon-yellow needle-like crystals of **2** up to 0.1 mm in the longest dimension were recovered. The products were filtered and washed with hexane. The resulting solution was colorless and transparent. The yield of the synthesis of **2** was 37% on the basis of Pb. The synthesis with the same reagents ratio and similar temperature/pressure conditions but not pH adjusted by NaOH results in formation of perfect orange hexagonal plates of $Pb(I,Br)_2$ and Pb(OH)I.[11]

*$Pb_{5.5}Si_{0.5}O_6Cl$ (**3**).* α-PbO (powder, ≥99.999%, Aldrich), SiO_2 (powder, ≥99.999%, Aldrich), and $PbCl_2$ (powder, 98%, Aldrich) reagents in ratio 1:0.5:5 were used to obtain single crystals of **3**. Large content of the last component is due to the usage of $PbCl_2$ as a flux in this synthesis. $PbCl_2$ was placed on the bottom of platinum crucible. The mixture of α-PbO and SiO_2 was ground in an agate mortar under acetone and after drying loaded into a platinum crucible on the $PbCl_2$ substrate and kept at 750 °C for 1 h in air, followed by cooling to 25 °C at a cooling rate of 9.5 °C/min. The product consisted of honey-yellow plate crystals of **3** in the mass of $Pb_3O_2Cl_2$[12] and unidentified amorphous residual. The same mixture cooled down to room temperature at a lower cooling rate of 7 °C/h results in the formation of transparent yellowish crystals of $Pb_3Si_2O_7$[13] and $PbSiO_3$.[14]

The electron-microprobe analyses (HITACHI-TM 3000) were performed for **1**–**3**. Qualitative electron microprobe analysis revealed no other elements, except Pb, Cl, and Ge (**1**); Pb, I, and Br (**2**); Pb, Si, and Cl (**3**) with the atomic number greater than 11 (Na).

Crystallographic Studies. Single crystals of the obtained compounds were mounted on thin glass fibers for X-ray diffraction analysis using Bruker APEX II DUO X-ray diffractometer with a microfocus X-ray tube operated with Mo Kα radiation at 50 kV and 40 mA. The data were integrated and corrected for absorption using a multiscan type model implemented in the Bruker programs *APEX* and *SADABS*. More than a hemisphere of X-ray diffraction data were collected for each crystal. Crystallographic information is summarized in Table 1. Atomic coordinates and additional structural information are provided in the Supporting Information (CIF).

RESULTS AND DISCUSSION

Phase **1** is a metastable high-temperature phase that can be obtained exclusively by rapid quenching of the lead–germanium oxyhalide melt. This method was employed previously[15] and proved to be efficient to obtain Pb phases with unusually complex structural architectures. The structure of **1** contains 7 symmetrically independent Pb sites. Pb(6) site is split into less occupied Pb6(A) and Pb6(B) sites. The coordination environments of the Pb atoms are variable in agreement with the presence of stereochemically active "lone pairs" on divalent lead cations. As it is typical for lead oxyhalides, halide ions and "lone pairs" on the Pb^{2+} cations associate in the same regions of the crystal structures. This phenomenon can be interpreted as a sign of the soft–soft attraction between halide ions and lone electron pairs known as halophilicity of the lone electron pairs. The structure of **1** contains one Ge site coordinated tetrahedrally by four O atoms with the average ⟨Ge–O⟩ bond length equal to 1.75 Å. The total number of oxygen sites is seven. The O(3), O(4), O(6), and O(7) sites are bonded to Ge, whereas other O atoms (O(1), O(2), O(5)) are tetrahedrally coordinated by Pb atoms, which results in formation of oxocentered OPb_4 tetrahedra (Figure 2). The average ⟨O–Pb⟩ distances within the OPb_4 tetrahedra are in the range 2.21–2.51 Å, which is in good agreement with the average value of 2.33 Å derived earlier.[7] There are five symmetrically independent Cl sites. The Cl(1) and Cl(2) atoms are

dx.doi.org/10.1021/ic402066h | *Inorg. Chem.* 2013, 52, 12799–12805

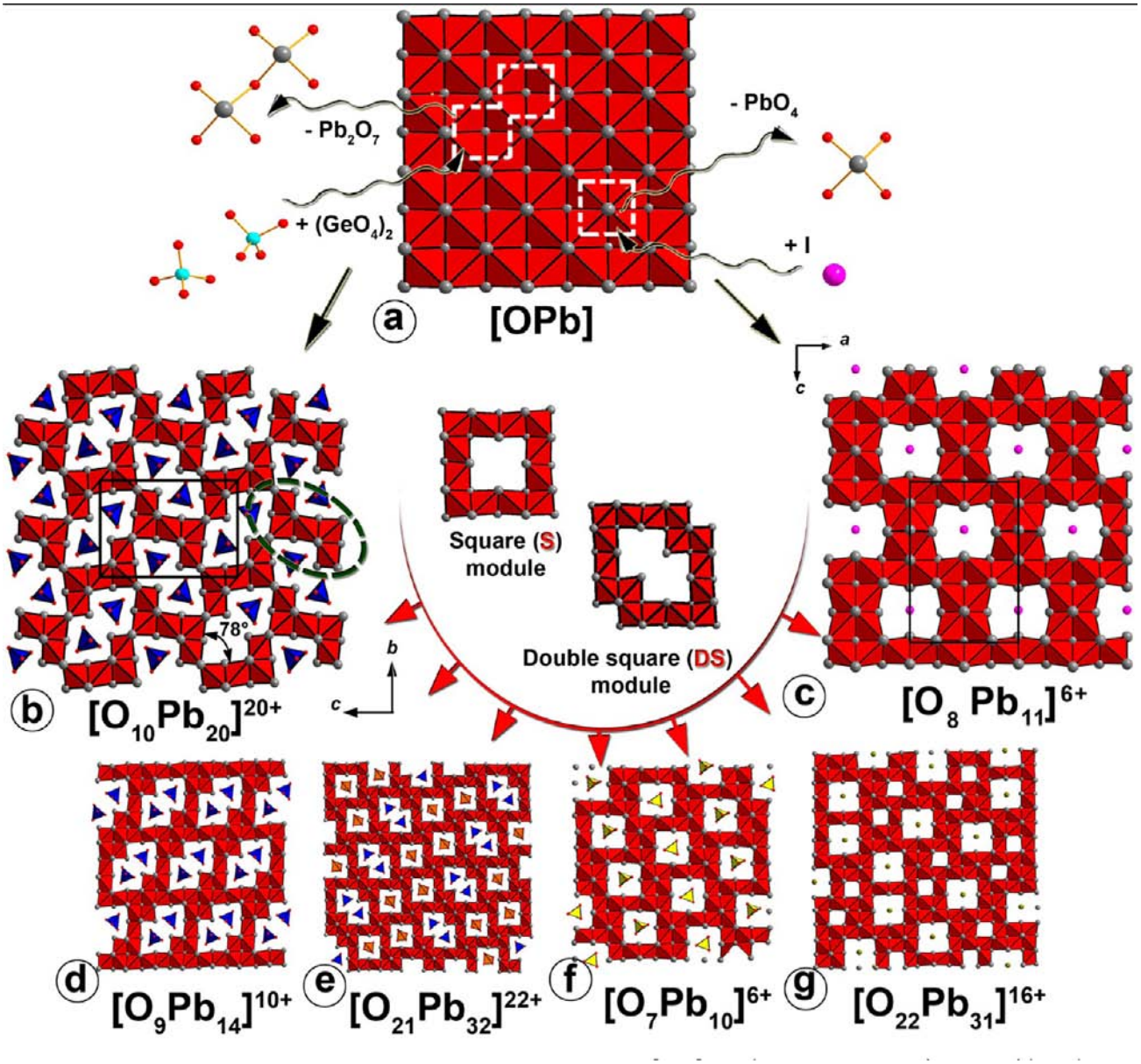

Figure 2. General scheme of formation of PbO-derivative layers from the defect-free [OPb] layer (red = OPb_4 tetrahedra) in α-PbO (a). *DS* (double square) modules and consequent $[O_{10}Pb_{20}]^{20+}$ layers (ξ angle 78.1(1)° is denoted) (b) in the structure of **1** are formed as a result of removal of Pb_2O_7 groups from the [OPb] layer and incorporation of two single GeO_4 tetrahedra. S (square) modules and consequent $[O_8Pb_{11}]^{6+}$ in the structure of **2** are formed by the removal of PbO_4 groups and incorporation of I atoms. S and *DS* modules also form the following 2*D* units in Pb oxyhalides: $[O_9Pb_{14}]^{10+}$ layer in the structure of kombatite (designations: blue = VO_4) (d), $[O_{21}Pb_{32}]^{22+}$ layer in the structure of hereroite (designations: blue = AsO_4, orange = mixed $(Si,As,V,Mo)O_4$) (e), $[O_7Pb_{10}]^{6+}$ layer in the structure of symesite (designations: yellow = SO_4) (f), $[O_{22}Pb_{31}]^{16+}$ layer in the structure of $Pb_{31}O_{22}X_{18}$ (X = Br, Cl) (designations: brown balls = Br^-). See the text for details.

coordinated more or less symmetrically by eight Pb atoms each, which is typical for Pb oxyhalides. In contrast, coordination of the Cl(3), Cl(4), Cl(5) sites is strongly distorted due to the presence of low-occupied and disordered Pb(6) and Pb(7) sites in their coordination spheres.

The structure of **1** (Figure 3b) belongs to the 1:1 type (Figure 1b) and consists of alternating PbO-type layers and mixed Pb−Cl sheets oriented parallel to (100). The PbO-type layer is a derivative of the [OPb] tetrahedral layer in α-PbO and can be obtained from the latter by removal of blocks of oxocentered tetrahedra. The GeO_4 tetrahedral anions locate in the cavities within the PbO-type layer (Figure 2b). The formula of the layer can be written as $[O_{10}Pb_{20}]^{20+}$. The vacancies within the $[O_{10}Pb_{20}]^{20+}$ in the structure of **1** have a shape of double square similar to those previously observed in natural minerals such as kombatite, $Pb_{14}(VO_4)_2O_9Cl_4$;[3c] sahlinite, $Pb_{14}(AsO_4)_2O_9Cl_4$;[3f] and hereroite, $[Pb_{32}O_{20}(O,\square)](AsO_4)_2((Si,As,V,Mo)O_4)_2Cl_{10}$.[3h] We denote this type of 7-fold module as *DS* (double square) (Figure 2). The *DS* modules in the structure if **1** are arranged in a way, which is drastically different from those observed in the structures of the minerals mentioned above. In fact, the $[O_{10}Pb_{20}]^{20+}$ layer found in the structure of **1** is unique within the class of lead oxyhalides and has not been observed previously. This layer can also be described as built up from *z*-like block (Figure 2b) of five oxocentered OPb_4 edge-sharing tetrahedra. The *Z*-like blocks are linked to each

dx.doi.org/10.1021/ic402066h | *Inorg. Chem.* 2013, 52, 12799−12805

Table 1. Crystal Structure Data for $Pb_3[O_{10}Pb_{20}](GeO_4)_4Cl_{10}$ (1), $[O_{16}Pb_{22}][OPb](OH)I_{10}(I,Br)(H_2O)$ (2), and $Pb_{5.5}Si_{0.5}O_6Cl$ (3)

	1	2	3
T (K)	120	120	120
radiation	Mo Kα	Mo Kα	Mo Kα
M_r (g mol^{-1})	728.28	1070	642.52
cryst syst	orthorhombic	orthorhombic	tetragonal
space group	*Cmca*	$Pmn2_1$	*I*4/*m*
a (Å)	28.352(19)	11.0697(11)	3.8897(7)
b (Å)	11.116(7)	15.5603(14)	3.8897(7)
c (Å)	16.513(11)	16.1335(16)	32.560(6)
V (Å^3)	5204(6)	2779.0(5)	492.45(15)
ρ_{calcd} (g cm^{-3})	7.436	7.670	8.666
μ (mm^{-1})	76.925	75.684	94.011
reflns collected	45 579	15 523	2085
indep reflns (R_{int})	6225 (0.1420)	5087 (0.0557)	315 (0.0431)
GOF	0.990	1.039	1.177
R1 [$I > 2\sigma(I)$]	0.0504	0.0386	0.0518
wR2	0.1122	0.0871	0.1391
R1 (all data)	0.0960	0.0455	0.0541
wR2	0.1338	0.0915	0.1418
largest diff peak and hole (e Å^3)	6.94, −4.379	3.139, −5.696	5.504, −3.182

other via Pb(1) atoms of the OPb_4 tetrahedra. Since these blocks are not fixed rigidly by edge linkage of tetrahedra [as, e.g., in the $[O_9Pb_{14}]^{10+}$ (Figure 2d) and $[O_{21}Pb_{32}]^{22+}$ (Figure 2e) layers], the $[O_{10}Pb_{20}]^{20+}$ layer is easily distorted. The distortion also occurs in order to accommodate comparatively large GeO_4 tetrahedra. The ξ angle in the *DS* module in **1** (Figure 2b) is 78.1(1)°, whereas ξ = 85.1(1)° and ξ = 87.1(1)° are much closer to the ideal value of 90° observed in the structures of kombatite and hereroite, respectively. The topological complexity of layers containing *DS* modules in minerals was evaluated previously using the method of square lattices.[3h,15] The VO_4 tetrahedra located in *DS* modules in kombatite are directed toward each other (Figure 3a). It is worth noting that kombatite belongs to the 2:1 type (Figure 1c). The same is observed in the structure of **1** for the GeO_4 tetrahedra. However, the interlayer spaces in **1** incorporate additional Cl and Pb atoms, which results in formation of the 1:1-type structure.

There are two types of halogen interlayers in the structure of **1** (Figure 3b,d,e). Interlayers of the first type contain defect-free ideal pseudotetragonal Cl sheets formed by the Cl(1) and Cl(2) atoms. This type of halogen sheets has been observed previously in many Pb oxyhalides.[3c,f,h,j] The defect-free pseudotetragonal *X* sheet (Figure 3d) in **1** can be considered as a parent substructure for all the halogen layer derivatives in the Pb oxyhalides. Interlayers of the second type contain the Cl(3), Cl(4), and Cl(5) sites together with low-occupied and disordered Pb(6) and Pb(7) sites (Figure 3e). This layer can be obtained from the ideal *X* sheet by substituting some Cl atoms by Pb. The distortion of *X*−Pb layer in **1** from the ideal *X* pseudotetragonal net is a result of the stereochemical activity of the lone electron pairs on the Pb^{2+} cations.

The structure of **1** and oxocentered $[O_{10}Pb_{20}]^{20+}$ block can be obtained from the ideal 1:1-type structure and the [OPb] layer according the following sequential transformations (Figure 2): (1) removal of Pb_2O_7 groups from the ideal defect-free [OPb] layer observed in α-PbO; (2) distortion of the resulting *DS* modules due to the presence of corner linkage between OPb_4 within the defect sheet; (3) incorporation of GeO_4 single tetrahedral units into *DS*-shaped cavities in the metal oxide matrix; (4) intrusion of the additional Pb atoms into the halogen interlayer.

Alkaline conditions for the synthesis of **2** were chosen in accordance with the previously reported pH values in the range of 4−9 suitable for formation of lead oxy-hydroxyhalide phases in natural and technological environments.[16] The high pH values for formation of synthetic layered Pb oxyhalides with defect PbO derivative sheets were also previously reported.[17]

There are 17 symmetrically independent Pb^{2+} cations in the structure of **2** with irregular and different coordination environments. The Pb−O bond lengths are in the range 2.19−2.87 Å, whereas the Pb−*X* (*X* = Br, I) bond lengths (all the Pb−I bond lengths ≤4.1 Å were taken into account due to the bond-valence requirements) vary from 2.96 to 4.08 Å. There are eight *X* sites occupied by the I atoms in the structure of **2**. The *X*(4) site has a mixed occupancy and is occupied by approximately 75% I and 25% Br, as confirmed by electron microprobe analysis.

The diversity and complexity of the oxygen atomic arrangements in **2** is remarkable. One of the O sites, OW(1), should be assigned to the O atom of the H_2O molecules. The O(7) atom belongs to the OH^- group that forms two O(7)−Pb(14) bonds of 2.371(7) Å each with the formation of the $(OH)Pb_2$ dimers. These dimers are typical for the Pb oxyhalides formed in aqueous environments.[17,18] The O(1)−O(4), O(6), and O(8)−O(10) sites are tetrahedrally coordinated by four Pb atoms each, thus forming OPb_4 oxocentered tetrahedra. The average ⟨O−Pb⟩ bond lengths in the tetrahedra are in the range 2.31−2.33 Å, which is in good agreement with the average value of 2.33 Å. The O(5) atom forms three short O−Pb bonds being at the center of the OPb_3 unit. Oxocentered OA_3 (A = metal) triangles are typical for bismuth oxysalts with additional oxygen atoms,[19] but have never observed previously in Pb oxyhalides. From the viewpoint of the bond-valence theory, the O_a−Pb bonds (O_a, additional oxygen atoms) are the shortest and therefore the strongest in the structure of **2**, which makes it reasonable to consider the Pb−O substructure consisting of OPb_4 tetrahedra and OPb_3 triangles as an independent structural unit interacting with X atoms through weak Pb−*X* (*X* = Br, I) bonds.

The topology of the oxocentered Pb−O structural unit is two-dimensional and can also be related to the [OPb] layer typical for PbO-derivative oxyhalides. The OPb_4 tetrahedra share common edges and corners to produce the novel $[O_8Pb_{11}]^{6+}$ layer depicted in Figure 2c. In contrast to the structure of **1**, the vacancies have a shape of a single square obtained by the removal of one PbO_4 group. Thus, the whole $[O_8Pb_{11}]^{6+}$ layer in the structure of **2** can be considered as constructed from the square (S) modules. The similar modules have been found in a number of natural[3e] and synthetic[15] complex Pb oxyhalides, but with different stacking sequences involved (Figure 2). The S modules in **2** are occupied by the I^- anions. Cavities of the same shape but occupied by Br^- were observed previously in $Pb_{31}O_{22}X_{18}$ (*X* = Br, Cl) (Figure 2g). The formula of the resulting oxocentered block designated as A in Figure 3f can be written as $([O_8Pb_{11}][OPb])^{6+}$ with the first part in square brackets designating the moiety formed by the OPb_4 tetrahedra, whereas the second part indicates 3-coordinated O atoms and the Pb atoms not participating in the OPb_4 tetrahedra. The $O(5)Pb_3$ triangles share common edges and corners with OPb_4 tetrahedra in the A block as shown in Figure 3f. The Pb(16) apex of the $O(5)Pb_3$ unit points in the direction of the *X* layer. The formula of the B block is $([O_8Pb_{11}]OH])^{5+}$. The structure of **2** is the first example of a layered Pb oxyhalide with compositionally different blocks arranged in a polytype-like arrangement. The interlayer in between the

dx.doi.org/10.1021/ic402066h | *Inorg. Chem.* 2013, 52, 12799−12805

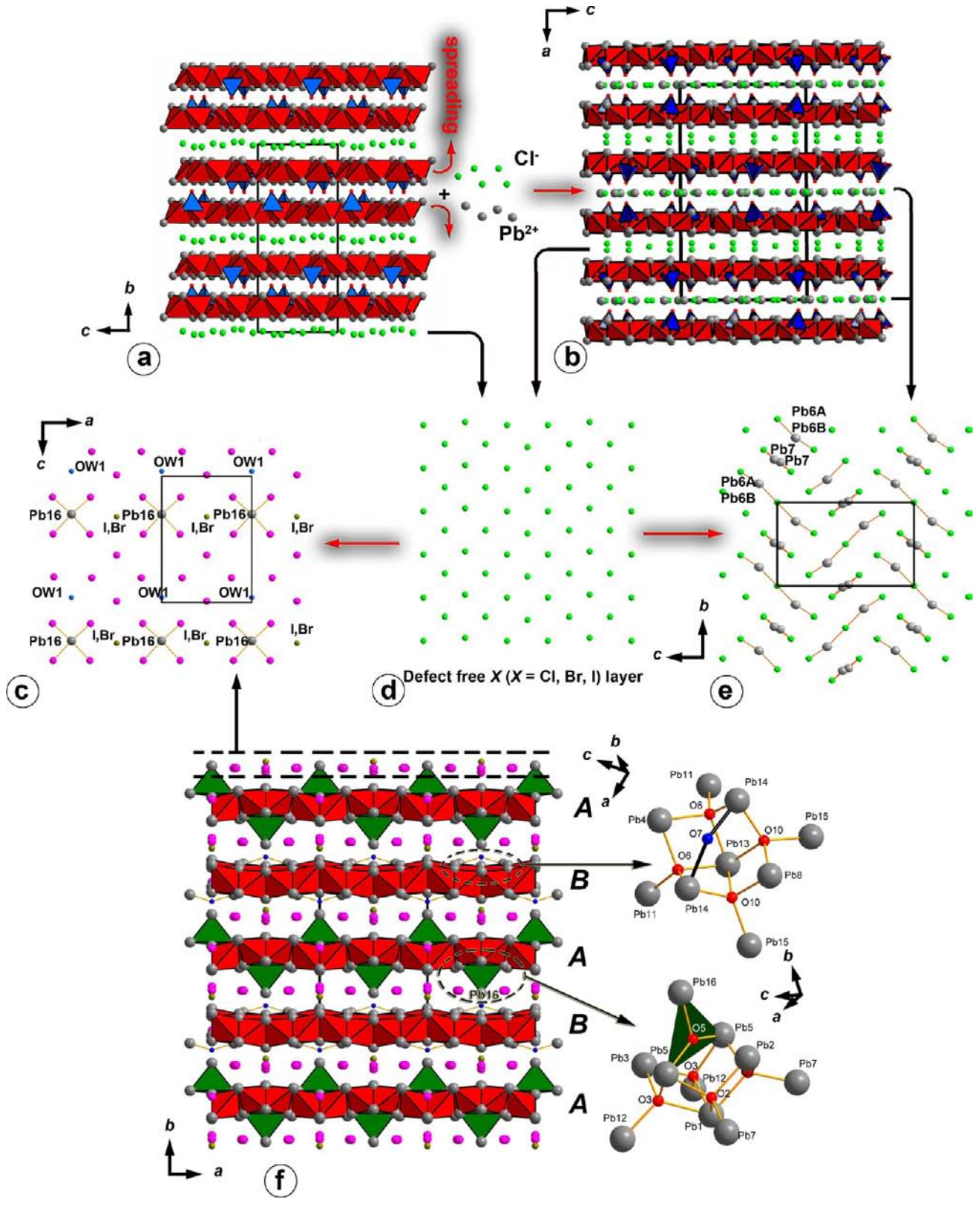

Figure 3. General projection of the crystal structure of kombatite along the *a* axis (a) and the structure of **1** along the *b* axis (b). Cl and Pb atoms are intruded in between the O−Pb with tetrahedral units (blue) directed toward each other [designations: blue = TO_4 (T = V or Ge), green balls = Cl, gray balls = Pb, red = OPb_4 tetrahedra]. The structure of **1** contains defect-free sheets of Cl atoms (d). I−Br−Pb−H_2O in **2** (c) and Pb−Cl sheets in **1** (e) are obtained by the replacement of some halogen atoms in ideal layer (d) and subsequent distortion. General projection of the crystal structure of **2** (f) with highlighted fragments showing the attachment of OPb_3 triangles in A layers and $OHPb_2$ dimers in B layers. See the text for details.

oxocentered 2D blocks in **2** is occupied by the I and Br atoms, and the H_2O molecules with "empty" spaces under or above the OH^- groups attached to the oxocentered B blocks (Figure 3c). This layer can be also obtained from the ideal defect-free *X* sheet described above in **1**.

dx.doi.org/10.1021/ic402066h | *Inorg. Chem.* 2013, 52, 12799−12805

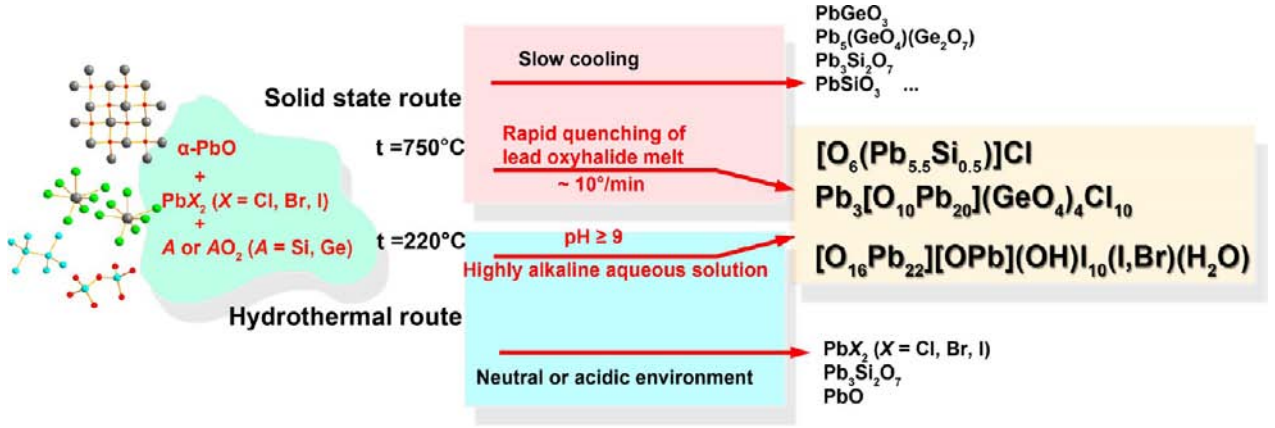

Figure 4. General strategy for the synthesis of complex α-PbO derivative Pb oxyhalides.

Rapid quenching of Si-containing Pb oxide chloride melt with considerable excess of $PbCl_2$ resulted in formation of the compound **3**. The structure of **3** contains three Pb sites (Figure 1d). The Pb(1) and Pb(2) sites have mixed occupation by the Pb^{2+} and Si^{4+} cations, whereas the Pb(3) site is fully occupied by Pb^{2+}. The Pb(3) site has a typical coordination of a PbO_4Cl_4 square antiprism. The Pb(1) and Pb(2) mixed cationic sites have only four short (Pb,Si)−O bonds in one coordination hemisphere, whereas the opposite hemisphere is occupied by the lone electron pairs. One symmetrically independent Cl site in the structure of **3** is 50%-occupied.

The OPb_4 and $O(Pb,Si)_4$ tetrahedra in **3** form continuous vacancy-free sheets depicted in Figure 2a. The $OPb(1)_4$ tetrahedra form the layer B (Figure 1d), whereas $OPb(2)_4$ and $OPb(3)_4$ comprise the layers A and C. Partial substitution of Pb^{2+} by Si^{4+} is necessary for the structure to be stable and is similar to the case observed in synthetic asisite, $Pb_7SiO_8Cl_2$.[20c] The ratio of the O−Pb blocks and *X* sheets in the structure of **3** is 3:1. This ratio has never been observed in the O−Pb Aurivillius phases[4] and structurally related minerals.[20]

CONCLUSION

As a result of this study, three novel Pb oxyhalides were obtained. Their structures belong to three principally different but related (Figures 2 and 3) 2D structure types with oxocentered OPb_4 tetrahedra as basic structural units. The 2D topologies of layers in the structures of **1** and **2** are unique. The structure of **3** is the first Pb oxyhalide with the 3:1 stacking sequence of the O−Pb blocks and halogen sheets. The compound **2** is a novel representative of lead oxyiodides, very few of which have been known to date. The structures of **1** and **2** are based upon the S and *DS* modules, which were known before to occur in the variety of mineral crystal structures. Natural Pb oxychloride is therefore a good example of a mineral that can be used as a guide and inspiration for the synthesis of novel compounds potentially demonstrating advanced materials properties.[21] We note that the structure of the $[O_{21}Pb_{32}]^{22+}$ layer in hereroite[3h] (Figure 2e) contains combination of the S and *DS* modules organized into alternating diagonal stripes. To date, synthetic compounds with combination of *DS* and S modules are unknown. Modular approach to the structures of complex inorganic phases attracted considerable attention[22] and proved to be the useful concept for rational design of novel families of inorganic compounds.[23] The structures of **1**−**3** show that this approach is also operational for complex Pb oxyhalide phases accommodating tetrahedral anions or large (I, Br) atoms. The dependence of the topology of the O−Pb layer upon the size of incorporating anions is remarkable and can be used for preparation of new layered inorganic compounds with novel structural architectures. These types of compounds have proved to have rich crystal chemistry and to be a fruitful garden for obtaining new compounds.

Phases **1** and **3** reported herein have been obtained by the rapid quenching of Pb oxyhalide melt. Crystal synthesis of lead oxyhalides is challenging because of multiple effects. The synthesis procedures are summarized in Figure 4. The "rapid quenching route" seems to be a very prospect for obtaining new PbO-derivative Pb oxyhalides with variety of additional cations for the tuning of different properties. Alkaline conditions are also suitable for obtaining Pb oxyhalides with high defect PbO-derivative layers as demonstrated by the synthesis of **2** from aqueous solutions. Further attempts of syntheses of Pb oxyhalides in $PbO-PbX_2-A_nO_m$ (A = metal) and $PbO-PbX_2-H_2O$ (*X* = Cl, Br, I) systems using a strategy represented in Figure 4 may result in the fabrication of novel compounds with unprecedented structural topologies. The type of the module in the structures of Pb oxyhalides obviously correlates with the size of incorporating anions: larger tetrahedra occupy the *DS* cavities, whereas smaller tetrahedra or single halogen atoms occupy smaller S cavities.

ASSOCIATED CONTENT

Supporting Information

X-ray crystallographic data in CIF format. This material is available free of charge via the Internet at http://pubs.acs.org.

AUTHOR INFORMATION

Corresponding Author

*E-mail: siidra@mail.ru.

Present Address

[†]The Drey, Allington Track, Allington, Salisbury SP4 0DD, Wiltshire, United Kingdom.

Notes

The authors declare no competing financial interest.

ACKNOWLEDGMENTS

This work was financially supported the Russian Federal Grant-in-Aid Program "Cadres" (agreement 8313), RFBR grant 12-05-31349, and by St. Petersburg State University through the internal grant 3.38.83.2012. Technical support by the SPbSU X-Ray Diffraction Resource Center is gratefully acknowledged.

REFERENCES

(1) (a) Ter Haar, G. L.; Bayard, M. A. *Nature* **1971**, *232*, 553−554. (b) Post, J.; Buseck, P. R. *Environ. Sci. Technol.* **1985**, *19*, 682−685. (c) Cziczo, D. J.; Stetzer, O.; Worringen, A. *Nat. Geosci.* **2009**, *2*, 333−336.

(2) (a) Matsumoto, H.; Miyake, T.; Iwahara, H. *Mater. Res. Bull.* **2001**, *36*, 1177−1184. (b) Sigman, M. B., Jr.; Korgel, B. A. *J. Am. Chem. Soc.* **2005**, *127*, 10089−10095. (c) Shan, Z.; Lin, X.; Liu, M.; Ding, H.; Huang, F. *Solid State Sci.* **2009**, *11*, 1163−1169. (d) Füldner, S.; Pohla, P.; Bartling, H.; Dankesreiter, S.; Stadler, R.; Gruber, M.; Pfitzner, A.; König, B. *Green Chem.* **2011**, *13*, 640−643. (e) Cherevatskaya, M.; Neumann, M.; Füldner, S.; Harlander, C.; Kümmel, S.; Dankesreiter, S.; Pfitzner, A.; Zeitler, K.; König, B. *Angew. Chem., Int. Ed.* **2012**, *51*, 4062−4066. (f) Siidra, O. I.; Krivovichev, S. V.; Armbruster, T.; Depmeier, W. *Inorg. Chem.* **2007**, *46*, 1523−1525. (g) Shu, J.; Ma, R.; Shao, L.; Shui, M.; Wang, D.; Wu, K.; Long, N.; Ren, Y. *Electrochim. Acta* **2013**, *102*, 381−387. (h) Aliev, A.; Olchowka, J.; Colmont, M.; Capoen, E.; Wickleder, C.; Mentre, O. *Inorg. Chem.* **2013**, *52*, 8427−8435.

(3) (a) Humphreys, D. A.; Thomas, J. H.; Williams, P. A.; Symes, R. F. *Mineral. Mag.* **1980**, *43*, 901−904. (b) Edwards, R.; Gillard, R. D.; Williams, P. A.; Pollard, A. M. *Mineral. Mag.* **1992**, *56*, 53−65. (c) Cooper, M. A.; Hawthorne, F. C. *Am. Mineral.* **1994**, *79*, 550−554. (d) Welch, M. D.; Criddle, A. J.; Symes, R. F. *Mineral. Mag.* **1998**, *62*, 387−393. (e) Welch, M. D.; Cooper, M. A.; Hawthorne, F. C.; Criddle, A. J. *Am. Mineral.* **2000**, *85*, 1526−1533. (f) Bonaccorsi, E.; Pasero, M. *Mineral. Mag.* **2003**, *67*, 15−21. (g) Krivovichev, S. V.; Turner, R.; Rumsey, M.; Siidra, O. I.; Kirk, C. A. *Mineral. Mag.* **2009**, *73*, 75−89. (h) Siidra, O. I.; Krivovichev, S. V.; Turner, R. W.; Rumsey, M. S.; Spratt, J. *Am. Mineral.* **2013**, *98*, 248−255. (i) Siidra, O. I.; Krivovichev, S. V.; Turner, R. W.; Rumsey, M. S.; Spratt, J. *Am. Mineral.* **2013**, *98*, 256−261. (j) Turner, R. W.; Siidra, O. I.; Krivovichev, S. V.; Stanley, C. J.; Spratt, J. *Mineral. Mag.* **2012**, *76*, 1247−1255.

(4) (a) Aurivillius, B. *Chem. Scripta* **1982**, *19*, 97−107. (b) Aurivillius, B. *Chem. Scr.* **1983**, *22*, 51−61.

(5) (a) Charkin, D. O. *Russ. J. Inorg. Chem.* **2008**, *53*, 1977−1996. (b) Zurbuchen, M. A.; Freitas, R. S.; Wilson, M. J.; Schiffer, P.; Roeckerath, M.; Schubert, J.; Biegalski, M. D.; Mehta, G. H.; Comstock, D. J.; Lee, J. H.; Jia, Y.; Schlom, D. G. *Appl. Phys. Lett.* **2007**, *91*, 033113−033115. (c) Zurbuchen, M. A.; Sherman, V. O.; Tagantsev, A. K.; Schubert, J.; Hawley, M. E.; Fong, D. D.; Streiffer, S. K.; Jia, Y.; Tian, W.; Schlom, D. G. *Appl. Phys. Lett.* **2010**, *107*, 024106−024117.

(6) (a) Boher, P.; Garnier, P.; Gavarri, J. R.; Hewat, A. W. *J. Solid State Chem.* **1985**, *57*, 343−350. (b) O'Keeffe, M.; Hyde, B. G. *Crystal Structures. I. Patterns and Symmetry*; Mineralogical Society of America: Chantilly, VA, 1996.

(7) Krivovichev, S. V.; Mentré, O.; Siidra, O. I.; Colmont, M.; Filatov, S. K. *Chem. Rev.* **2013**, *113*, 6459−6535.

(8) (a) Krivovichev, S. V.; Armbruster, T.; Depmeier, W. *J. Solid State Chem.* **2004**, *177*, 1321−1332. (b) Charkin, D. O.; Lightfoot, P. *Am. Mineral.* **2006**, *91*, 1918−1921.

(9) Nozik, Yu.Z.; Maksimov, B. A.; Fykin, L. E.; Dudarev, V.Ya.; Garashina, L. S.; Gabrielyan, V. T. *Zh. Strukt. Khim.* **1978**, *19*, 731−733.

(10) Kay, M. I.; Newnham, R. E.; Wolfe, R. W. *Ferroelectrics* **1975**, *9*, 1−6.

(11) Naesaenen, R. *Suom. Kemistil.* **1966**, *39B*, 105−108.

(12) Siidra, O. I.; Krivovichev, S. V.; Armbruster, T.; Depmeier, W. *Z. Kristallogr.* **2008**, *223*, 204−211.

(13) Petter, W.; Harnik, A. B.; Keppler, U. *Z. Kristallogr.* **1971**, *133*, 445−458.

(14) Krivovichev, S. V.; Burns, P. C. *Zapiski Vserossijskogo Mineralogicheskogo Obshchestva* **2004**, *5*, 70−76.

(15) Krivovichev, S. V.; Siidra, O. I.; Nazarchuk, E. V.; Burns, P. C.; Depmeier, W. *Inorg. Chem.* **2006**, *45*, 3846−3848.

(16) Edwards, R., Gillard, R. D., Williams, P. A. and Pollard, A. M. *Mineral. Mag.* **1992**, *56*, 53-65.

(17) Krivovichev, S. V.; Burns, P. C. *Can. Mineral.* **2006**, *44*, 515−522.

(18) (a) Krivovichev, S. V.; Burns, P. C. *Eur. J. Mineral.* **2002**, *14*, 135−139. (b) Krivovichev, S. V.; Burns, P. C. *Eur. J. Mineral.* **2001**, *13*, 801−809. (c) Krivovichev, S. V.; Burns, P. C. *Solid State Sci.* **2001**, *3*, 455−459. (d) Siidra, O. I.; Krivovichev, S. V.; Depmeier, W. *Geol. Ore Deposits* **2008**, *50*, 801−805.

(19) (a) Bedlivy, D.; Mereiter, K. *Am. Mineral.* **1982**, *67*, 8833−8840. (b) Ridkosil, T.; Srein, V.; Fabry, J.; Hybler, J.; Maximov, B. A. *Can. Mineral.* **1992**, *30*, 215−224. (c) Mereiter, K.; Preisinger, A. *Österr. Akad. Wiss. Math.—Naturwiss. Kl. Sitzungsb.* **1986**, *123*, 79−81.

(20) (a) Welch, M. D. *Mineral. Mag.* **2004**, *68*, 247−254. (b) Rouse, R. C.; Peacor, D. R.; Dunn, P. J.; Criddle, A. J.; Stanley, C. J.; Innes, J. *Am. Mineral.* **1988**, *73*, 643−650. (c) Lepore, G. O.; Welch, M. D. *Mineral. Mag.* **2010**, *74*, 269−275.

(21) Depmeier, W. *Cryst. Res. Technol.* **2009**, *10*, 1122−1130.

(22) Ferraris, G.; Makovicky, E.; Merlino, S. *Crystallography of Modular Materials*; Oxford University Press: Oxford, U.K., 2004.

(23) Kabbour, H.; Cario, L.; Danot, M.; Meerschaut, A. *Inorg. Chem.* **2006**, *45*, 917−922.